






HP1c regulates development and gut homeostasis by suppressing Notch signaling through Su(H)

Jin Sun^{1,2,†} , Xia Wang^{1,3,†}, Rong-Gang Xu^{1,†}, Decai Mao^{1,4,†}, Da Shen^{1,†}, Xin Wang^{5,†}, Yuhao Qiu^{1,6,†}, Yuting Han^{1,†} , Xinyi Lu^{1,†}, Yutong Li^{1,†}, Qinyun Che¹, Li Zheng¹, Ping Peng^{1,6}, Xuan Kang⁷, Ruibao Zhu^{1,6}, Yu Jia^{1,6}, Yinyin Wang⁸, Lu-Ping Liu¹, Zhijie Chang⁸, Jun-Yuan Ji⁹, Zhao Wang¹⁰, Qingfei Liu¹⁰, Shao Li^{5,*} , Fang-Lin Sun^{7,**}  & Jian-Quan Ni^{1,11,***} 

Abstract

Notch signaling and epigenetic factors are known to play critical roles in regulating tissue homeostasis in most multicellular organisms, but how Notch signaling coordinates with epigenetic modulators to control differentiation remains poorly understood. Here, we identify heterochromatin protein 1c (HP1c) as an essential epigenetic regulator of gut homeostasis in *Drosophila*. Specifically, we observe that HP1c loss-of-function phenotypes resemble those observed after Notch signaling perturbation and that HP1c interacts genetically with components of the Notch pathway. HP1c represses the transcription of Notch target genes by directly interacting with Suppressor of Hairless (Su(H)), the key transcription factor of Notch signaling. Moreover, phenotypes caused by depletion of HP1c in *Drosophila* can be rescued by expressing human HP1 γ , suggesting that HP1 γ functions similar to HP1c in *Drosophila*. Taken together, our findings reveal an essential role of HP1c in normal development and gut homeostasis by suppressing Notch signaling.

Keywords *Drosophila* development; gut homeostasis; HP1c; Notch signaling pathway; Su(H)

Subject Categories Chromatin, Transcription & Genomics; Development; Signal Transduction

DOI 10.15252/embr.202051298 | Received 10 July 2020 | Revised 1 January 2021 | Accepted 13 January 2021 | Published online 17 February 2021

EMBO Reports (2021) 22: e51298

Introduction

In addition to the primary functions of digestion and absorption, intestinal epithelium plays an important role in resistance to tissue injury, inflammation, and other adverse conditions. Disruption of intestinal homeostasis can lead to diseases such as gastrointestinal tumors. In *Drosophila*, intestinal stem cells (ISCs) reside along the midgut to maintain tissue homeostasis (Micchelli & Perrimon, 2006; Ohlstein & Spradling, 2006). An ISC divides asymmetrically, giving rise to one ISC (for self-renewal) and one committed progenitor enteroblast (EB), which further differentiates into either an absorptive enterocyte (EC) or a secretory enteroendocrine cell (ee cell) (Lemaitre & Miguel-Aliaga, 2013).

A variety of signaling pathways, including Notch, JAK/STAT, Wnt, EGFR/Ras, Hippo, Hedgehog, and BMP, are involved in regulating the self-renewal and differentiation of ISCs under either normal homeostasis or stress conditions (Biteau *et al.*, 2011; Jiang & Edgar, 2011; Pasco *et al.*, 2015). Of these signaling pathways, the highly conserved Notch is critical in maintaining intestinal homeostasis (Ohlstein & Spradling, 2007; Fre *et al.*, 2011). Accordingly, dysregulation of Notch signaling causes abnormal intestinal cell lineage development and uncontrolled intestinal cell growth. Specifically, reduced Notch signaling in ISCs disrupts stem cell differentiation, resulting in fewer ECs and more ee cells, as well as the aggregation of ISCs and the formation of gut tumors (Micchelli & Perrimon, 2006; Ohlstein & Spradling, 2006; Perdigoto *et al.*, 2011). Conversely, hyperactive Notch signaling forces ISCs to differentiate

1 Gene Regulatory Lab, School of Medicine, Tsinghua University, Beijing, China

2 Shandong First Medical University & Shandong Academy of Medical Sciences, Jinan, China

3 School of Life Sciences, Peking University, Beijing, China

4 Sichuan Academy of Grassland Science, Chengdu, China

5 Institute for TCM-X, MOE Key Laboratory of Bioinformatics/Bioinformatics Division, BNRIST, Department of Automation, Tsinghua University, Beijing, China

6 Tsinghua University-Peking University Joint Center for Life Sciences, Beijing, China

7 Research Center for Translational Medicine at East Hospital, School of Life Sciences and Technology, Advanced Institute of Translational Medicine, Tongji University, Shanghai, China

8 State Key Laboratory of Membrane Biology, School of Medicine and the School of Life Sciences, Tsinghua University, Beijing, China

9 Department of Molecular and Cellular Medicine, College of Medicine, Texas A&M Health Science Center, College Station, TX, USA

10 School of Pharmaceutical Sciences, Tsinghua University, Beijing, China

11 Tsingdao Advanced Research Institute, Tongji University, Qingdao, China

*Corresponding author. E-mail: shaoli@mail.tsinghua.edu.cn

**Corresponding author. E-mail: sf@tongji.edu.cn

***Corresponding author. E-mail: nijq@mail.tsinghua.edu.cn

†These authors contributed equally to this work

into ECs, leading to the loss of ISCs and ee cells (Ohlstein & Spradling, 2007; Goulas *et al.*, 2012).

The Notch signaling pathway is initiated by a ligand–receptor interaction between two adjacent cells. The receptor Notch then goes through two steps of a proteolytic cleavage process, resulting in the release of the intracellular domain of the Notch protein (NICD), which translocates into the nucleus. Subsequently, NICD binds to the CSL-type DNA-binding transcription factor and recruits transcription coactivators to regulate the expression of Notch target genes. In *Drosophila*, the CSL-type DNA-binding protein Su(H) (Suppressor of Hairless) orchestrates transcription cofactors such as Hairless, CtBP, and Groucho to control the transcription of Notch target genes (Mummery-Widmer *et al.*, 2009; Saj *et al.*, 2010; Guarani *et al.*, 2011; Mulligan *et al.*, 2011; Maier *et al.*, 2013; Contreras-Cornejo *et al.*, 2016; Han *et al.*, 2016; Nagel *et al.*, 2016). However, due to many interconnections with other signaling pathways and complicated outcomes, the mechanisms by which these transcription cofactors, particularly epigenetic factors, regulate the expression of Notch target genes in the nucleus remain unclear.

The heterochromatin protein 1 (HP1) family is highly conserved epigenetic proteins in eukaryotes, and their functional diversity is further achieved through multiple variants (Canzio *et al.*, 2014). There are five HP1 variants in *Drosophila*, HP1a–e, with HP1a being extensively studied as a silencing epigenetic factor (Vermaak & Malik, 2009; Canzio *et al.*, 2014), and HP1c as a euchromatic protein (Kwon & Workman, 2011). Previous results showed that HP1c interacts with zinc finger-containing DNA-binding proteins WOC (without children) and ROW (relative of WOC) to form a complex (Font-Burgada *et al.*, 2008; Abel *et al.*, 2009), which may be involved in RNA polymerase II pausing (Kwon *et al.*, 2010; Kessler *et al.*, 2015). Therefore, HP1c has been generally recognized as a promising epigenetic regulator of gene transcription (Kwon & Workman, 2011). However, the role of HP1c in development and gene expression regulation remains poorly understood.

Here, we report our analyses of the key role of HP1c in regulating development and intestinal homeostasis through Notch signaling in *Drosophila*. Our results indicate that HP1c physically interacts with Su(H) to suppress the transcription of Notch target genes.

Results

HP1c-specific phenotypes resemble Notch perturbations

To elucidate functional genomic abnormalities underlying human gut tumorigenesis, we conducted genomic disorder analyses including disease-related gene prediction and differential gene expression analyses. We identified 178 highly conserved high-risk genes in both human colorectal and gastric cancers by using CIPHER (average top 5% in the rank list) (Fig 1A and B, Dataset EV1), a state-of-the-art network-based prediction for prioritizing disease genes in a genome-wide scale (Wu *et al.*, 2008). To validate the functions and conserved roles of these genes in gut homeostasis *in vivo*, we chose to use *Drosophila* as a model organism. *Drosophila* gut is an ideal system to study the molecular mechanisms of tumorigenesis because of its relative simplicity in comparison with mammalian systems, the availability of sophisticated genetic tools, and the functional

conservation of genes and signaling pathways. Notch signaling plays a critical role in driving ISCs to replenish the loss of absorptive and secretory cells in both *Drosophila* and mammals, and dysregulated Notch signaling is closely associated with gut homeostasis (Koch & Radtke, 2007; Geissler & Zach, 2012; Nowell & Radtke, 2017). Therefore, to determine whether any of these 178 high-risk genes are involved in regulating Notch signaling, we generated *Drosophila* transgenic RNAi lines against their human homologs.

Given that the development of *Drosophila* notum bristles is sensitive to Notch signaling, we performed a phenotypic screen to test whether depleting the fly homologs of these high-risk genes affects the development of the mechanosensory bristles on the notum using *pnr-Gal4*, which is specifically expressed in the central region of the notum (Fig 1A and B, and Dataset EV1). Compared to the control carrying one anterior scutellar (aSC) bristle (see dotted square in Fig 1C), gain of Notch signaling with CRISPR/dCas9-based transcriptional activation system (Jia *et al.*, 2018), or loss of Notch signaling repressor dSir2 (Mulligan *et al.*, 2011), caused additional aSC bristles (double-bristles) in the same region (Figs 1D and E, and EV1A). Thirty-five genes show the gain of bristles, loss of bristles, or hair cell duplication phenotypes; however, most of them are involved in DNA replication, protein synthesis, or signaling pathways such as Ras, Wnt. One of the remaining genes, HP1c, which is homologous to human HP1 γ (i.e., Chromobox 3, CBX3), is known as transcriptional regulators, but the developmental role is unclear. Interestingly, from this genetic screen we observed that depleting HP1c, which is homologous to human HP1 γ (i.e., Chromobox 3, CBX3), resulted in ectopic aSC bristles in the flies (Figs 1F and EV1A, Dataset EV1). This effect resembles the phenotypes caused by Notch activation and dSir2 mutation. To further validate the effects of HP1c on aSC bristles, we generated an HP1c null mutant fly using the CRISPR/Cas9 system (Ren *et al.*, 2013; Ren *et al.*, 2014; Ren *et al.*, 2017). Consistent with HP1c depletion, 70% of HP1c null mutant flies also displayed extra aSC bristles (Figs 1G and EV1A). To exclude potential off-target effects, we performed rescue experiments and found that the expression of wild-type HP1c can completely rescue the ectopic aSC bristle phenotype caused by either depletion or loss of HP1c (Fig EV1B–D). These observations revealed a novel function of HP1c in regulating aSC bristle development, indicating the possibility that HP1c might interact with Notch signaling to control aSC bristle development similarly to dSir2.

Given that Notch signaling and dSir2 also regulate wing morphogenesis in *Drosophila* (Mulligan *et al.*, 2011), we wondered whether this was the case for HP1c. Using the *MS1096-Gal4* line, which is expressed in the entire wing imaginal disk, we observed that gain of Notch signaling caused ectopic veins from the distal fourth and fifth longitudinal veins and disrupted posterior cross veins (PCV) (Fig 1H and I). Similar phenotypes were observed in approximately 80% of the wings from dSir2 mutants (Fig 1K and L), which is consistent with the previous report (Mulligan *et al.*, 2011). Interestingly, almost all of the flies with either the HP1c depletion or HP1c mutation displayed ectopic veins from the distal of the fourth and fifth longitudinal veins and broken PCV (Fig 1J and M). These phenotypes also resemble the effects of gain of Notch signaling or loss of dSir2, implying a similar function for HP1c and dSir2 in negatively modulating Notch signaling during notum bristle and wing development.

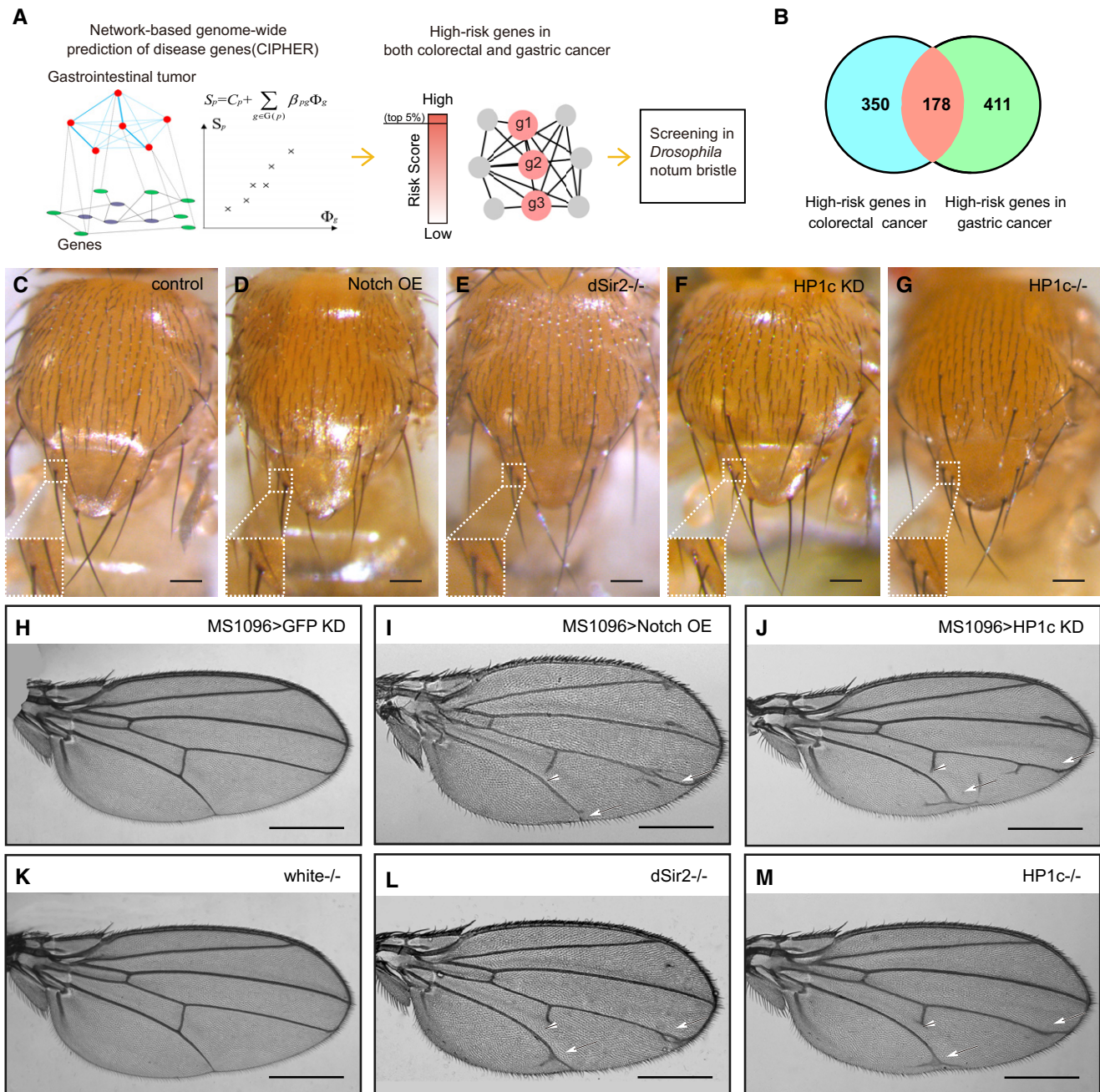


Figure 1. HP1c is involved in Notch-dependent *Drosophila* notum bristle and wing development.

- A** Workflow of the network-based analysis *in silico* and functional screen *in vivo*.
- B** The number of high-risk genes (DIOP score ≥ 5) in colorectal cancer and gastric cancer from genome-wide prediction (total: 17,903 genes).
- C-G** Resembling the phenotype caused by Notch overexpression (D) or dSir2 mutation (E), HP1c knockdown (F), and mutant (G) flies also exhibit supernumerary anterior scutellar (aSC) bristles on the notum, as indicated by the enlarged views in the left bottom panels. Scale bars, 100 μ m.
- H-M** Compared with control flies (H and K), HP1c knockdown (J) and mutant (M) flies exhibit an ectopic vein at the distal of L4 and L5 (arrows) and a broken posterior cross vein (arrowhead), which is similar to the phenotype caused by Notch overexpression (I) and dSir2 mutant (L). Scale bars, 500 μ m.

HP1c, as well as Notch signaling, regulates *Drosophila* gut homeostasis

Considering that HP1 γ is identified as a potential high-risk gene in human colorectal and gastric cancers (Fig 1 and Dataset EV1) and

that Notch signaling plays a critical role in gut homeostasis (Ohlstein & Spradling, 2007; Fre *et al*, 2011), we asked whether HP1c, the *Drosophila* homolog of HP1 γ , plays any role in regulating gut homeostasis. To avoid potential effects on the early developmental stage, we depleted HP1c in a temporal and spatial manner

using the temperature-sensitive *esg-Gal4*, *UAS-GFP*; *tub-Gal80^{ts}* system (hereafter referred to as *esg^{ts}*) in gut progenitor cells (Michelli & Perrimon, 2006), which allowed us to deplete HP1c in both ISCs and EBs and label them by GFP. To further distinguish ISCs, EBs, and ee cells, *Su(H)Gbe-lacZ* reporter was chosen to mark EBs by lacZ antibody, and anti-Prospero labeled ee cells in red.

Compared to control (Fig 2A), we observed that depletion of HP1c in midgut significantly reduced the number of ISCs that were

only marked by GFP (Fig 2B and EV2A). To detect whether the loss of stem cells because of hypoproliferation or apoptosis, we performed immunostaining using the specific antibodies against mitotic marker-H3S10p and apoptotic marker caspase 3, and the results show no obvious difference between the wild-type flies and HP1c KD or mutant flies (Fig EV2B–E), suggesting apoptosis and proliferation do not play an essential role to reduce the number of stem cells. Closer examination revealed that, in the wild-type, most

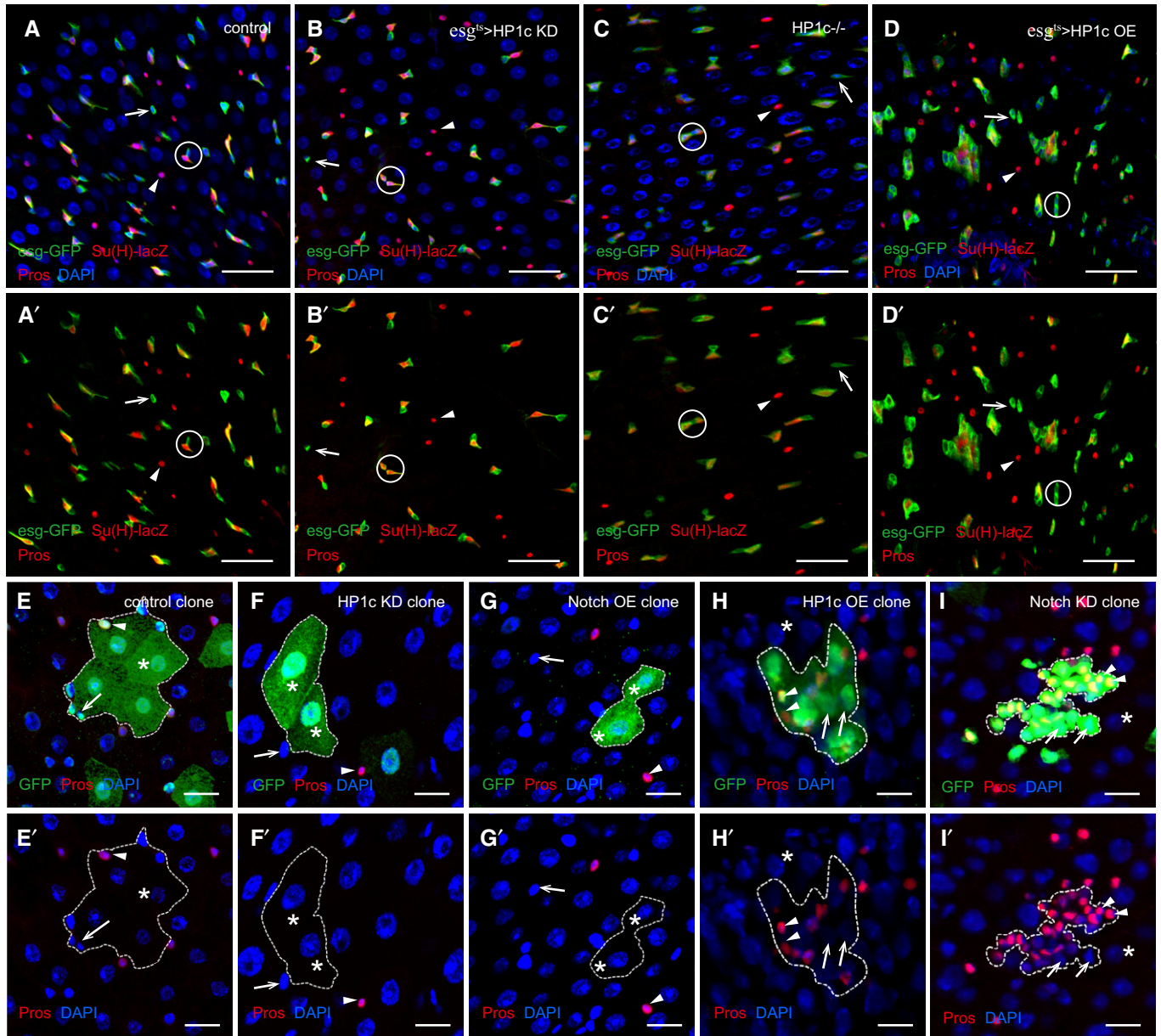


Figure 2. HP1c, as well as Notch signaling, regulates *Drosophila* gut homeostasis.

A–D The posterior midguts of 10-day-old control (A), HP1c knockdown (B), HP1c null mutant (C), and HP1c overexpression flies (D). Arrows mark ISCs; arrowheads mark ee cells; and circles mark ISC-EB, EB-EB, or ISC-ISC nests. ISCs were visualized with *esg-GFP* alone, EBs were stained with both *esg-GFP* and *Su(H)-lacZ*, while ee cells were labeled by *Pros* and DNA was marked by *DAPI*. Scale bars, 30 μ m.

E–I Confocal images of the posterior midgut clones of the indicated genotypes, marked by *GFP* (dotted lines). Arrows mark ISCs/EBs; arrowheads mark ee cells; and asterisks mark ECs. DNA was visualized with *DAPI* and ee cells were stained with *Pros*. Scale bars, 10 μ m.

if not all ISC-EB nests (pairwise ISC-EB) contain one ISC and one EB (labeled by solid circle in Fig 2A) as expected. However, in the HP1c-depleted progenitor cells, the expected ISC-EB nests often carry two EBs (EB nest; Figs 2A and B, and EV2A), suggesting that HP1c depletion triggers ISC differentiation, thus reducing the number of ISCs. In addition, the number of ee cells, marked by Prospero expression, is also significantly reduced (Figs 2A and B, and Fig EV2A), suggesting that HP1c depletion promotes ISCs to differentiate into ECs, but not ee cells. Similar to HP1c depletion using RNAi, midgut in *HP1c* mutant also contains significantly reduced numbers of ISCs and ee cells, with an increased number of EB nests (Figs 2A and C, and EV2A). These observations show that reduction or loss of HP1c promotes the differentiation of ISCs into EC cells.

To further validate the role of HP1c in gut homeostasis, we overexpressed HP1c in midgut using *esg^{ts}* and observed that higher levels of HP1c increased the numbers of both ISCs and ee cells (Figs 2D and EV2A). Interestingly, unlike the ISC-EB nests found in control, or the EB nests observed in reduction or loss of HP1c (Fig 2B), most nests in HP1c overexpression contain two ISCs (Fig 2D), which we designated as the ISC nest. This observation suggests that HP1c negatively regulates the differentiation of ISCs. Taken together, these results reveal a novel and important role of HP1c in regulating ISC differentiation, which may explain why its human homologous gene HP1 γ is identified as one of the top high-risk genes in both colorectal and gastric cancers.

Similar to the phenotypes caused by HP1c overexpression, depletion of Notch in midgut using *esg^{ts}* also increased the numbers of both ISCs and ee cells (Figs 2D and EV2F and G), whereas gain of Notch signaling caused a phenotype resembling HP1c depletion (Figs 2B and C, and EV2F and H). Together with the phenotypes analyzed in the development of aSC bristles and wing veins, these genetic and cell biological analyses imply a role for HP1c in Notch signaling.

To precisely determine the similarity between HP1c and Notch signaling in regulating ISC differentiation, we tracked the changing of clone cells by generating GFP-marked RNAi/OE clones using the FLP-out system in the midgut (Sun et al, 2015). Compared to the control, which carried large-nuclear ECs and small-nuclear progenitors and ee cells within each clone, we found that most of the GFP⁺ clone cells were only ECs in both HP1c depletion and Notch activation flies and grew by fewer than two cells in number (Figs 2E–G and EV2I and J). Conversely, clones of either overexpression of HP1c or depletion of Notch increased the numbers of small-nuclear progenitor cells and ee cells (Figs 2E and H, I, and EV2I and J). These results further demonstrate the same roles of HP1c and Notch signaling in regulating ISC differentiation.

HP1c genetically suppresses Notch signaling

Activation of the transmembrane Notch receptor by its ligands from the neighboring cells triggers a proteolytic event resulting in the release of NICD, which then enters into the nucleus and binds to the transcription factor Su(H), thereby turning on the transcription of Notch target genes (Mummery-Widmer et al, 2009; Saj et al, 2010; Contreras-Cornejo et al, 2016). Given that HP1c is best known to function as an epigenetic factor in the nucleus, the afore-described similarities between HP1c and Notch signaling in the genetic and cell biological analyses prompted us to test whether HP1c modulates

Notch signaling in the nucleus. We therefore asked whether overexpression of HP1c could rescue the phenotypes generated by Notch activation in midgut. Notch activation in *Drosophila* gut triggered by *esg^{ts}* reduces the number of both ISCs and ee cells, often showing EB nests (Figs 3A and B, and EV3A), while overexpression of HP1c increases the number of ISCs and ee cells (Figs 3A and C, and EV3A), suggesting the antagonistic relationship between HP1c and Notch signaling in the differentiation of ISCs. Interestingly, a simultaneous increase in Notch and HP1c significantly rescued the defects in ISC differentiation (Figs 3D and EV3A), suggesting that HP1c suppresses Notch signaling in regulating ISCs.

To further validate the role of HP1c in suppressing Notch signaling, we performed a phenotypic analysis using the *Drosophila* wing. *Notch* heterozygous mutant flies exhibited notched wings (arrowheads) and thickening of the L5 vein (arrow) (Fig 3E and F), and *Delta* heterozygous mutant flies showed a knotted L5 vein (arrow, Fig 3G), whereas the wings from *HP1c* heterozygous mutant flies were all the same as wild type (Fig 3H). To examine whether HP1c can modify the vein phenotypes caused by Notch signaling in the *Drosophila* wing, we partially reduced HP1c by recombination of a *HP1c* heterozygous mutant with either *Notch* or *Delta* heterozygous mutant flies. Interestingly, this strongly suppressed the wing defects of both *Notch* (Fig 3H and I) and *Delta* (Fig 3J) heterozygous mutant flies. Moreover, we also tested whether HP1c overexpression can rescue the vein phenotypes and the abnormal gene transcription caused by Notch activation; again, we observed that the defect of wings and gene transcription were all back to normal when overexpressing HP1c in the *Notch* OE background (Fig EV3B–E). This suppression of phenotypes caused by Notch perturbation further supports the genetic role of HP1c in negatively regulating Notch signaling.

HP1c associates with and represses Notch target genes

Since HP1c was reported to be involved in the regulation of gene transcription (Kwon et al, 2010; Kwon & Workman, 2011), we decided to investigate whether HP1c binds to the promoter regions of Notch target genes. For this, we performed the chromatin immunoprecipitation coupled with quantitative PCR (ChIP-qPCR) assay using cultured *Drosophila* S2 cells. As a positive control, we observed a significant enrichment of HP1c on the promoter of *pgm* gene (Fig 4A), which is a well-known HP1c target gene (Kessler et al, 2015). We also observed strong enrichment of HP1c on the promoters of several well-characterized Notch target genes, including *E(spl)m2*, *E(spl)m β* and *Hairy* (Fig 4A). These results suggest that HP1c associates with Notch target genes.

In parallel, we performed an *in vivo* chromatin profiling assay, known as the DamID (DNA adenine methyltransferase identification) method (Marshall et al, 2016). Specifically, we created Dam-HP1c by fusing Dam to the C terminus of HP1c and used sole Dam as the control. Compared to the Dam control, the signal intensity is significantly increased from Dam-HP1c in genes including *pgm*, *E(spl)m2*, and *Hairy* (Fig EV3F). These results further confirm the association of HP1c with Notch target genes.

Next, we asked whether depletion of HP1c affects the transcription of Notch target genes. We performed reverse transcription-quantitative PCR (RT-qPCR) using wing disks when HP1c was depleted by MS1096-Gal4 driver. As shown in Fig 4B, the expression of Notch

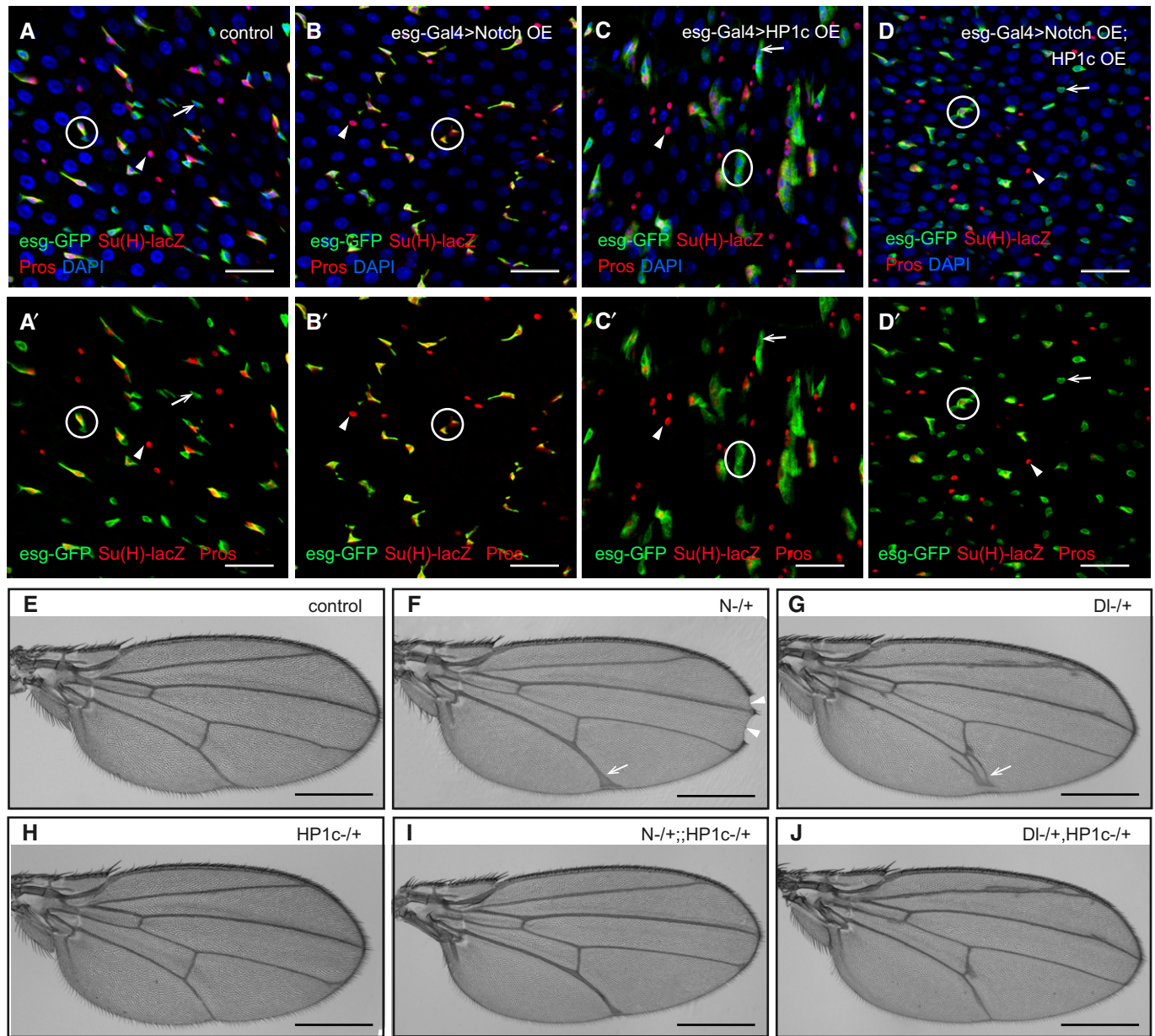


Figure 3. HP1c genetically represses the Notch signaling pathway.

A–D Compared with the control (A) flies, posterior midguts of Notch OE flies exhibit decreased ISCs and ee cells (B), while HP1c OE flies show increased ISCs and ee cells (C), and the phenotype of Notch OE can be rescued by HP1c OE (D). Arrows mark ISCs; arrowheads mark ee cells; and circles mark ISC-ISC, ISC-EB, or EB-EB nests. ISCs were visualized with *esg-GFP* alone; EBs were stained with both *esg-GFP* and *Su(H)-lacZ*, while ee cells were labeled by *Pros* and DNA was marked by DAPI. Scale bars, 30 μm.

E–J Images of wings from flies with the indicated genotypes. Arrows mark the ectopic veins at L5, and arrowheads mark the classical notched wing. Scale bars, 500 μm.

target genes such as *E(sp1)m2*, *HLHm5* and *Hairy* is significantly increased in HP1c-depleted wing disks compared to the control. Similarly, the transcription of these Notch target genes in wing disks from the *HP1c* null mutants is also significantly increased (Fig 4B), indicating the repressive role of HP1c with regard to Notch target genes. Moreover, to directly visualize the role of HP1c in suppressing the expression of Notch target genes, we generated a GFP reporter and analyzed the effects of HP1c on the expression of GFP under the

control of a Notch response element (NRE, containing four *Su(H)* binding sites). Specifically, we depleted HP1c in the posterior compartment of the wing disk (marked with RFP in Fig 4C) using the *engrailed-Gal4* (*en-Gal4*) driver. Compared with *white* control knock-down, depleting HP1c resulted in a dramatic upregulation of GFP fluorescence intensity (arrow, Fig 4C and D) and expansion of the GFP signal (arrowhead, Fig 4D), further supporting the negative role of HP1c in regulating Notch signaling *in vivo*.

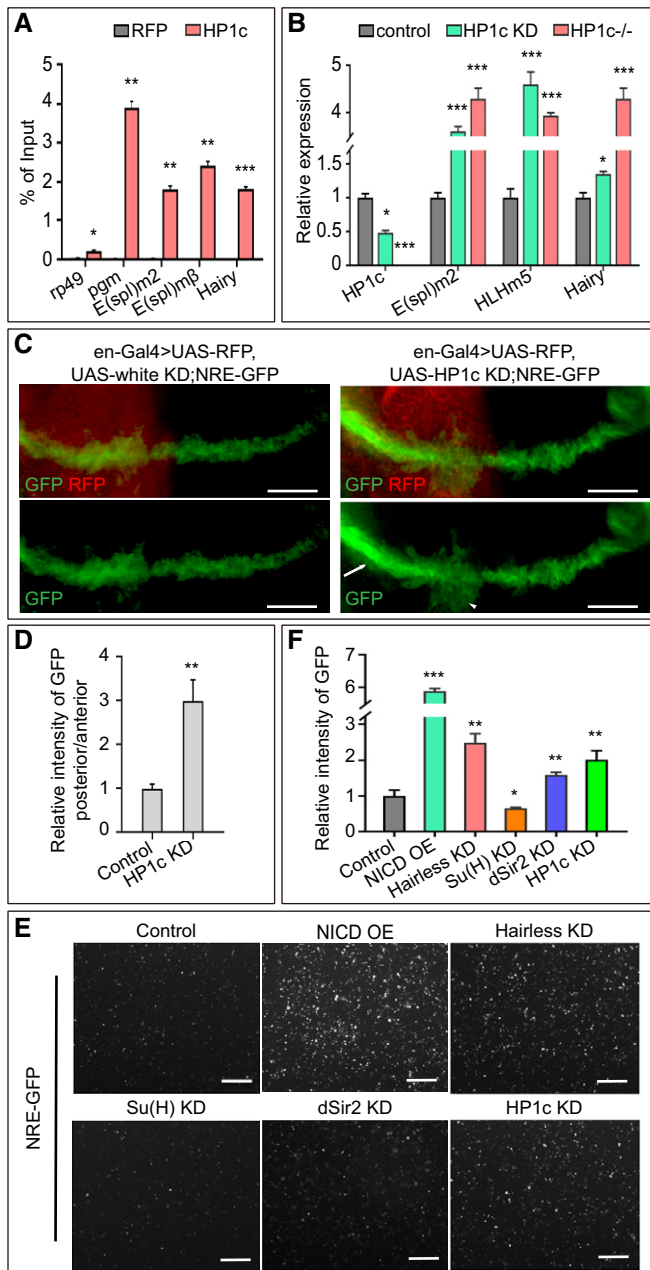


Figure 4. HP1c represses Notch target genes at the transcriptional level.

- A** ChIP-qPCR results show the association of HP1c with Notch target genes compared to RFP control. The amount of immunoprecipitated DNA in each sample is represented as signal relative to the total amount of input chromatin (equivalent to 1). Error bars indicate SEM. $n = 3$ technical replicates. Data are evaluated with two-tailed Student's *t*-test (* $P < 0.05$, ** $P < 0.01$, *** $P < 0.001$).
- B** RT-qPCR analysis determined the expression of Notch target genes when HP1c was depleted ($n = 3$ technical replicates, mean \pm s.d.). Data are evaluated with two-tailed Student's *t*-test (* $P < 0.05$, *** $P < 0.001$).
- C** Immunostaining result of *Drosophila* wing disk when control or HP1c was KD by en-Gal4, which knocked down target gene in RFP marked region, and HP1c KD caused upregulation (arrow) and expansion (arrowhead) of GFP signal under the control of a Notch response element (NRE) that the GFP fluorescence intensity represents the activity of Notch signaling. Scale bars, 20 μ m.
- D** Quantification of results in C showing that the relative GFP intensity in HP1c KD wing disks is about threefold higher than that in control ($n = 5$ biological replicates, mean \pm s.d.). Data are evaluated with Student's *t*-test (** $P < 0.01$).
- E, F** NRE-GFP signals of S2 cells carrying NICD OE, Hairless KD, Su(H) KD, dSir2 KD and HP1c KD (E), and the statistical results (F) ($n = 4$ biological replicates, mean \pm s.d.). Data are evaluated with two-tailed Student's *t*-test (* $P < 0.05$, ** $P < 0.01$, *** $P < 0.001$). Scale bars, 200 μ m.

interestingly, depleting HP1c further activated Notch signaling caused by overexpression of NICD on the NRE-luciferase reporter, while overexpression of HP1c had the opposite effect (Fig EV3H), which further supports the notion that HP1c functions as a repressor of the Notch signaling pathway *in vitro*. Taken together, these results show that HP1c directly associates with Notch target genes and represses the transcription of them *in vitro* and *in vivo*.

HP1c interacts with Su(H), the core transcription factor of Notch signaling

To define the molecular mechanism of how HP1c suppresses the expression of Notch target genes, we decided to test whether HP1c physically interacts with the core components of the Notch signaling pathway, including Notch, NICD, Mam (Mastermind), Hairless, and Su(H). For this, we performed the yeast two-hybrid assay and used HP1c as the bait and the other proteins as the prey. Strikingly, HP1c interacts with Su(H), but not other components of the Notch signaling pathway (Fig 5A). This observation was further validated by using full-length Su(H) as bait and HP1c as the prey (Fig 5A). These results suggest a direct interaction between HP1c and Su(H).

Next, we mapped the specific domains mediating the interactions between HP1c and Su(H). Like other HP1 family members, HP1c is characterized by two prominent domains: the chromodomain (CD) that normally binds to H3K9me and the chromoshadow-domain (CSD) that mediates protein–protein interactions through homodimerization (Fig 5B; Eisenberg & Elgin, 2000). Su(H) possesses three domains involved in mediating protein–DNA or protein–protein interactions: LAG1, BTB, and CTD (Fig 5B; Contreras-Cornejo *et al*, 2016). We have observed that full-length HP1c (as bait) specifically interacts with the BTB domain of Su(H), while full-length Su(H) (as bait) interacts with the CSD domain but not the CD domain of HP1c (Fig 5C). Furthermore, the CSD domain of HP1c interacts with the BTB domain of Su(H) (Fig 5C). These data further support the direct interaction between the HP1c CSD and Su(H) BTB domains.

To validate the effects of HP1c on the expression of Notch target genes *in vitro*, we analyzed the expression of NRE-GFP in cultured *Drosophila* S2 cells. Overexpression of NICD or depletion of Hairless, a major repressor of Notch signaling, significantly increased the expression of NRE-GFP, whereas depleting the transcription factor Su(H) significantly reduced the expression of the NRE-GFP reporter (Fig 4E and F). These observations are consistent with the role of NICD, Hairless, and Su(H) in regulating Notch signaling as previously described (Fre *et al*, 2011; Aster *et al*, 2017) and also proved the efficiency and sensitivity of our reporter. Interestingly, depleting either HP1c or dSir2 increases the expression of NRE-GFP by about twofold (Fig 4E and F), which is consistent with our phenotypic analyses. In addition, we generated an NRE-luciferase reporter and similar observations were obtained (Fig EV3G). Most

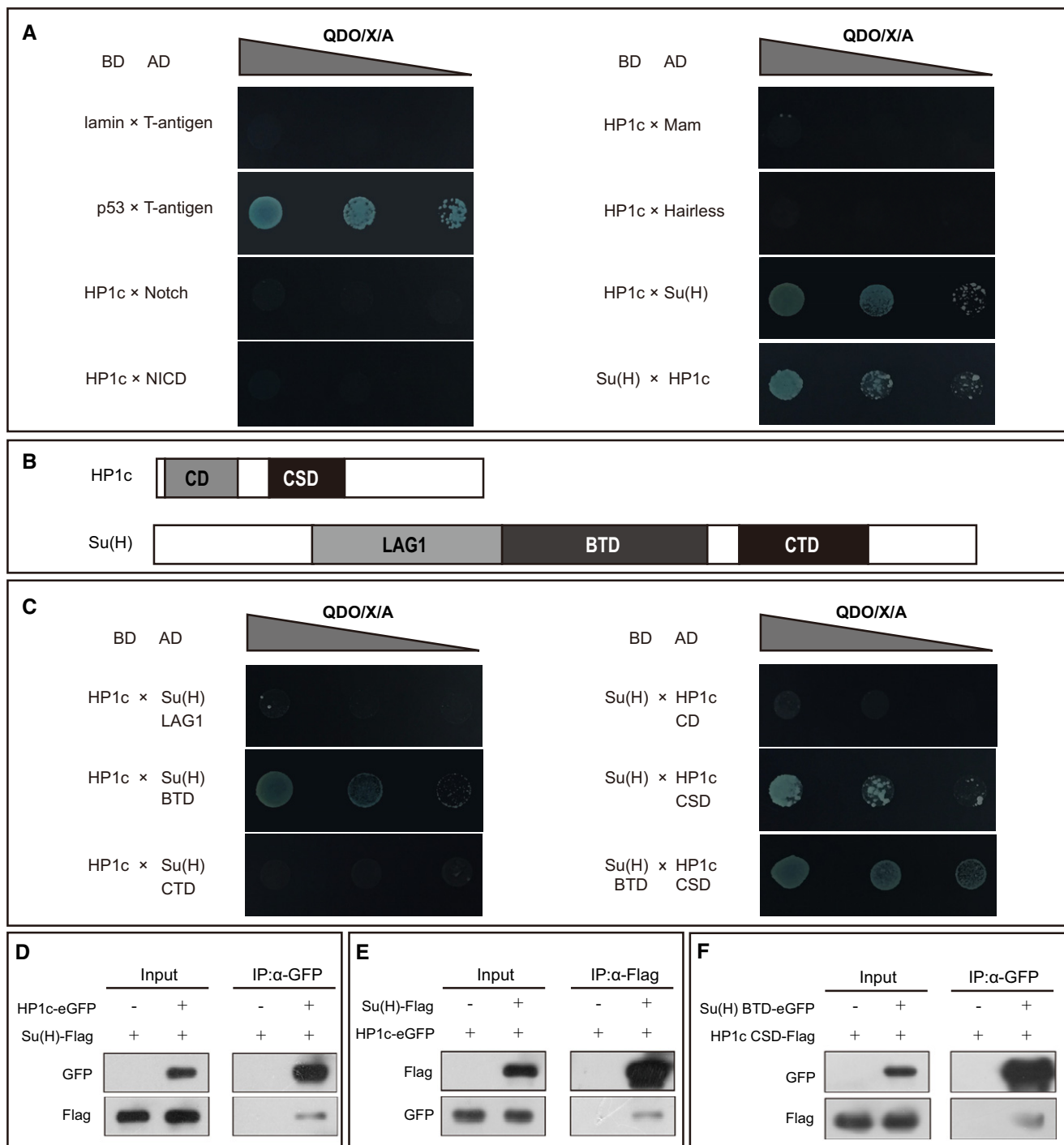


Figure 5. HP1c interacts with Su(H), the core transcription factor of Notch signaling.

- A** Yeast two-hybrid analysis identified that Su(H) is the only Notch signaling key component that interacts with HP1c, while lamin mated with T-antigen was used as negative control and p53 mated with T-antigen as positive control. The interactions between HP1c and Su(H) were confirmed in both orientations. (BD: binding domain, AD: activation domain, QDO/X/A: quadruple dropout medium: SD/-Ade/-His/-Leu/-Trp supplemented with X-a-Gal and Aureobasidin A).
- B** The main functional domains of HP1c and Su(H).
- C** The CSD domain of HP1c and the BTB domain of Su(H) are responsible for the interaction by yeast two-hybrid analysis.
- D, E** The interaction between HP1c and Su(H) is further confirmed through co-immunoprecipitation (Co-IP). Plasmids expressing HP1c-eGFP and Su(H)-flag were transfected into S2 cells. Immunoprecipitation and Western blotting were performed with the indicated antibodies.
- F** Plasmids expressing HP1c CSD domain and Su(H) BTB domain were transfected into S2 cells. Immunoprecipitation and Western blotting were performed with the indicated antibodies.

To test whether HP1c interacts with Su(H) *in vivo*, we performed co-immunoprecipitation (co-IP) experiments using eGFP-tagged HP1c co-transfected with Flag-tagged Su(H) in cultured S2 cells. As shown in Fig 5D, eGFP-tagged HP1c can indeed co-immunoprecipitate (co-IP) with Flag-tagged Su(H). Conversely, Flag-tagged Su(H) can co-IP with eGFP-tagged HP1c (Fig 5E). Remarkably, this approach also shows that the eGFP-tagged BTD domain of Su(H) can efficiently co-IP with the Flag-tagged CSD domain of HP1c protein (Fig 5F). Moreover, we performed another co-IP using S2 cells transfected with Flag-tagged Su(H) since we did not have a good Su(H) antibody available. As shown in Fig EV3I, the endogenous protein HP1c can be efficiently co-immunoprecipitated with Flag-tagged Su(H). All these data are consistent with the results from the yeast two-hybrid analyses, supporting that HP1c directly interacts with Su(H).

HP1c associates with Notch target genes in a Su(H)-dependent manner

To further determine the relationship between HP1c and Su(H) *in vivo*, we performed immunostaining of the polytene chromosome from the larval salivary glands. HP1c is widely distributed along the polytene chromatin, except in the heterochromatic region densely stained by DAPI (Fig 6A). Interestingly, Su(H) showed a similar pattern and largely co-localized with HP1c (Fig 6A). In summary, the association of HP1c with Notch target genes seen in the ChIP and DamID assays, the interaction with Su(H) based on both yeast two-hybrid and co-IP experiments, as well as the co-localization cytological experiment demonstrate that HP1c physically interacts with Su(H) *in vivo*, to repress Notch target genes.

Since Su(H) has a DNA-binding domain, the association of HP1c with Notch target genes might require Su(H). To test this, we performed ChIP-qPCR analysis to determine whether there was a change in HP1c on Notch target genes after Su(H) depletion. As expected, depleting Su(H) strongly reduced the enrichment of HP1c (Fig 6B), indicating that the association of HP1c with Notch target genes depends on the physical interaction with Su(H). To further explore the performance of HP1c when Notch signaling was activated, we performed ChIP-qPCR assay to detect the changing of HP1c on Notch target genes after overexpressing NICD. Surprisingly, more HP1c accumulates on Notch target genes than controls (Fig. 6C), suggesting a model that with the increasing Su(H) on Notch target genes when Notch signaling is activated (Gomez-Lamarca *et al*, 2018), more HP1c are simultaneously recruited to Notch target genes by Su(H) to form a feedback loop, thus to prevent the hyper-activation of Notch signaling.

Based on the previous report, the chromodomain has the highest affinity for the H3K9me, and the association is essential for gene silencing (Lachner *et al*, 2001; Bannister *et al*, 2001). To examine whether H3K9me can recruit HP1c on notch targeting genes through chromodomain, we conducted ChIP-qPCR experiment. Specifically, HP1c and HP1c mutant where the chromodomain was deleted were all tagged with flag and expressed in S2 cells; we collected the cells and performed ChIP-qPCR assay. Interestingly, the enrichment of HP1c mutant is slightly increased on notch target genes rather than reduction (Fig 6D–E), suggesting without chromodomain, the association on Notch target genes from HP1c mutant is more accessible than intact HP1c, and further supporting our conclusion that the binding of HP1c on notch target genes requires the interaction

between the chromo shadow domain and Su(H), while it is independent of the chromodomain that mediates the interaction between HP1c and H3K9me.

Human HP1 γ has conserved roles in regulating Notch signaling

There are five HP1 variants (HP1a–e) encoded by different genes in *Drosophila*. HP1a, HP1b, and HP1c are ubiquitously expressed, while HP1d and HP1e are mainly expressed in the reproductive system, in a tissue-specific manner. Since HP1c negatively regulates Notch signaling through interaction with Su(H) based on genetics and biochemical assay, we wonder whether this function is specific among the HP1 family. From the expression level, protein structure, and even the cellular localization, HP1b is as very similar as HP1c; however, in contrast to the HP1c KD, HP1b KD did not affect the number of ISCs/EBs in the midgut (Fig EV4A–D), and HP1b null mutant also showed normal wing (Fig 7A and B), suggesting the distinct function of HP1b from HP1c. In addition, the *HP1b* and *HP1c* double mutant flies (genotype: *HP1b*^{-/-}; ; *HP1c*^{-/-}) were viable and fertile, and the phenotypes resembled that of *HP1c* mutant flies (Fig 7C and D), indicating no redundancy between them. Furthermore, *HP1b* mutant also failed to rescue the vein phenotype caused by *Notch* mutant (Fig 7E and F). These observations indicate that HP1b is not involved in modulating Notch signaling, and support the specific role of HP1c in the Notch signaling pathway.

Since human HP1 γ is the HP1c homolog and is identified as a high-risk gene in both human colorectal and gastric cancers (Fig 1A and B, Dataset EV1), we want to know whether HP1 γ plays a conserved role in regulating Notch signaling in *Drosophila*. First, we performed a genetic complementary assay in the development of *Drosophila* notum bristles. Consistent with previous experiments, HP1c KD in the notum resulted in ectopic aSC bristles, while simultaneous overexpression of HP1 γ fully rescued this phenotype (Fig 7G–I), suggesting that HP1 γ functions as similar as HP1c in *Drosophila*. To further verify the similar role of human HP1 γ as *Drosophila* HP1c in Notch pathway regulation, we next analyzed the phenotypes in the *Drosophila* midgut. As we expected, the reduction of both ISCs and ee cells caused by HP1c depletion was also fully rescued by the overexpression of HP1 γ (Fig 7J–M), further supporting the conserved role of HP1c from *Drosophila* to human. Altogether, HP1c specifically suppresses Notch signaling and this role is conserved in human HP1 γ .

Discussion

Notch signaling plays critical roles in regulating cell differentiation and proliferation during normal development of multicellular organisms, and dysregulated Notch signaling causes abnormal development and a wide variety of human diseases including cancers (Koch & Radtke, 2007; Geissler & Zach, 2012; Nowell & Radtke, 2017). Despite decades of extensive studies, the mechanisms of how Notch target genes are controlled in the nucleus by different transcription cofactors, particularly epigenetic factors, remain not fully understood. In this study, we identified the epigenetic regulator HP1c in *Drosophila*, the human homolog being HP1 γ , as a negative regulator of Su(H)-dependent transcription of Notch target genes. Based on

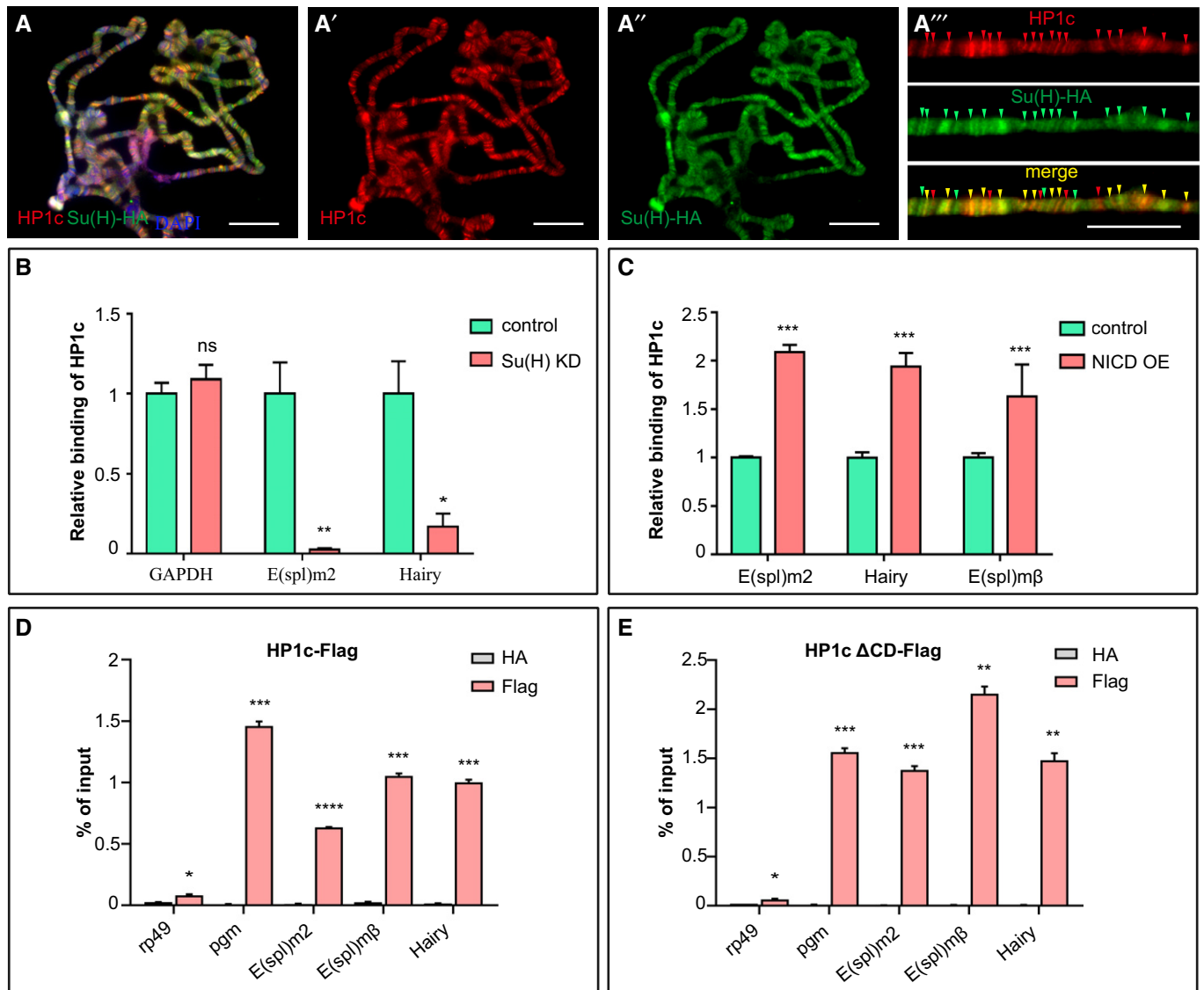


Figure 6. HP1c associates with Notch target genes in a Su(H)-dependent manner.

A Confocal images of the polytene chromatin show strong co-localization of HP1c and Su(H), with enlarged images are also shown. Arrowheads in (A'') indicate HP1c (red) and Su(H) (green) signals, while yellow arrowheads indicate co-localizations. Scale bars, 20 μ m.

B The relative binding of HP1c with Notch target genes when Su(H) KD using ChIP-qPCR analysis ($n = 3$ technical replicates, mean \pm s.d.). Data are evaluated with two-tailed Student's t -test (* $P < 0.05$, ** $P < 0.01$).

C The relative binding of HP1c on Notch target genes when NICD OE using ChIP-qPCR analysis ($n = 3$ technical replicates, mean \pm s.d.). Data are evaluated with two-tailed Student's t -test (** $P < 0.001$).

D, E ChIP-qPCR results show the association of Flag-tagged HP1c and chromodomain depleted HP1c mutant (HP1c Δ CD) with Notch target genes. The amount of immunoprecipitated DNA in each sample is represented as signal relative to the total amount of input chromatin (equivalent to 1). HA antibody is used as a control. Error bars indicate SEM. $n = 3$ technical replicates. Data are evaluated with two-tailed Student's t -test (* $P < 0.05$, ** $P < 0.01$, *** $P < 0.001$, **** $P < 0.0001$).

our data, we proposed a model to explain how HP1c suppresses the transcription of Notch target genes (Fig EV5). In the absence of NICD, both HP1c and other repressors interact with different domains of Su(H) to coordinately repress the transcription of Notch target genes. Loss of HP1c affects the balance of this transcriptional repression, resulting in the mild activation of Notch signaling (Fig EV5). When NICD is present, it interacts with Su(H) to compete

with and replace other transcription repressors, the loss of repressors in Su(H) complex will trigger the transcription of Notch target genes, and then require more Su(H) accumulate on Notch target genes (Gomez-Lamarca *et al*, 2018), where the increasing of HP1c to prevent the hyper-activation of Notch signaling. If we reduce HP1c in this circumstance, it can further active the transcription of Notch target genes to hyper-transcription status (Fig EV5).

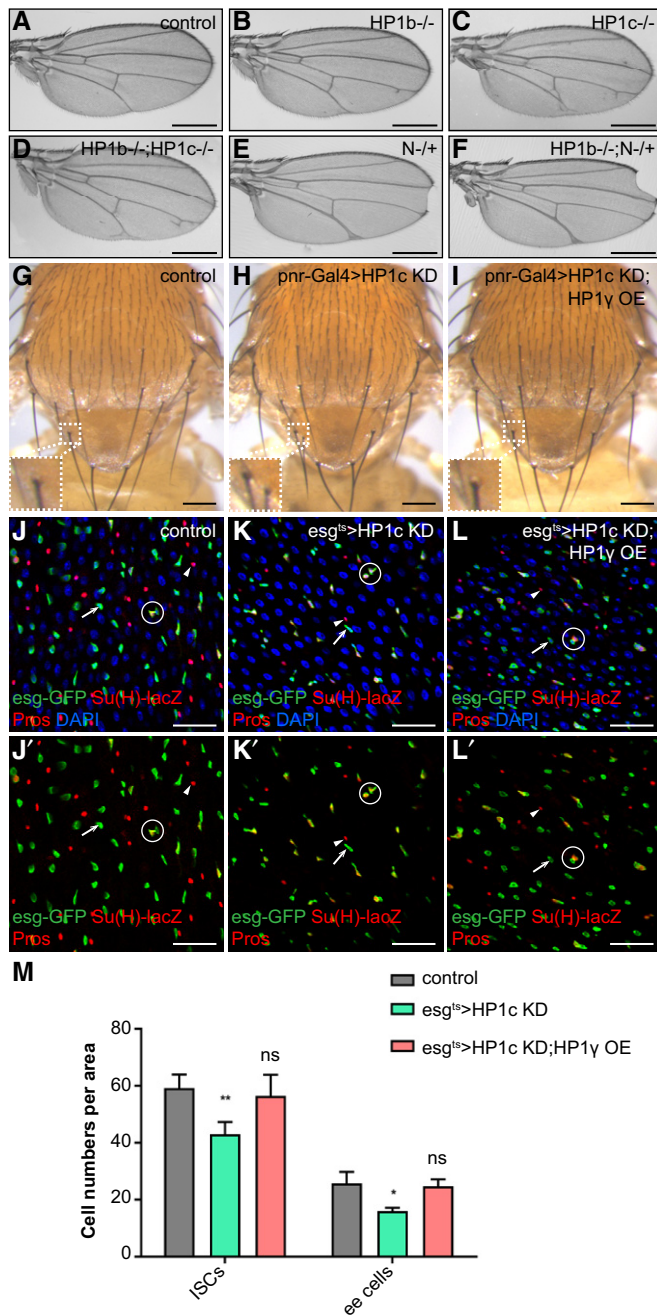


Figure 7. Human HP1 γ plays conserved roles in intestine homeostasis and development.

A–F HP1b null mutant did not show ectopic vein in the wing and failed to genetically interact with HP1c and Notch. Scale bars, 500 μ m.

G–I The notum bristle phenotype caused by HP1c depletion can be rescued by human homolog HP1 γ OE, as indicated by the enlarged views in the left bottom panes. Scale bars, 100 μ m.

J–L The ISC differentiation defect produced by HP1c KD can be rescued by human homolog HP1 γ OE. Scale bars, 30 μ m.

M Statistical results of the number of ISCs and ee cells per unit area (200 μ m \times 200 μ m) in (D–F). More than twenty-five midguts were examined for each group. Error bars indicate SEM. Data are evaluated with two-tailed Student's *t*-test (**P* < 0.05, ***P* < 0.01).

It has been reported previously that HP1c can positively regulate gene expression by recruiting the FACT histone chaperone complex and the absence of HP1c reduces the transcription of heat-shock genes (Kwon *et al*, 2010). However, we found that HP1c functions as a transcriptional repressor to regulate Notch target genes *in vivo* for the following reasons. First, the reduction or loss of HP1c results in defects in *Drosophila* development and intestinal homeostasis that resemble the phenotypes caused by activation of Notch signaling and the transcriptional repressor dSir2 mutant. Second, increasing HP1c phenocopies the effects caused by loss of Notch signaling. Third, our ChIP and RT-qPCR analyses have revealed that HP1c directly inhibits the expression of Notch target genes. Fourth, *in vitro* and *in vivo* assays using the NRE-GFP or NRE-luciferase reporter show that HP1c negatively regulates the transcription of Notch target genes in a manner similar to known transcriptional repressors such as Hairless and dSir2. Mechanistically, we have found that the effects of HP1c on the expression of Notch target genes are dependent on Su(H), the key transcription factor of Notch signaling. Furthermore, our biochemical analyses show that the CSD domain of HP1c directly interacts with the BTB domain of Su(H). Taken together, our genetic, biochemical, and cytological analyses suggest that HP1c functions as a transcriptional repressor that directly suppresses the transcription of Notch target genes *in vivo*, thereby revealing multifaceted and context-specific functions of HP1c during development.

On the other hand, we also detected whether another number of HP1 family, HP1b, plays the similar role with HP1c. However, although both HP1b and HP1c have CD and CSD domains, and both mainly bind to euchromatin regions (Ryu *et al*, 2014), they function distinctively, only HP1c specifically modulates Notch signaling, while HP1b not, both from analysis of HP1b RNAi and null mutant. To address whether HP1c specifically regulates Notch signaling, not EGFR, we performed the rescue experiment. As shown in Fig EV4E–H, the reduction of HP1c did not change the vein phenotype caused by EGFR knockdown, supporting the specific role of HP1c in Notch pathway regulation.

In addition, our analyses of the human HP1 γ suggest that in *Drosophila*, same as HP1c, HP1 γ negatively regulates Notch signaling. Considering that HP1 γ is a high-risk gene for gastrointestinal inflammation and tumorigenesis and downregulated Notch signaling highly associates with tumor in many tissues (Reedijk *et al*, 2005; Koch & Radtke, 2007; Geissler & Zach, 2012; Bedogni, 2014; Nowell & Radtke, 2017), the detailed molecular mechanisms and potential mechanistic conservation in mammals need to be further studied in the future.

Materials and Methods

Drosophila strains and transgenic information

All flies were raised on standard cornmeal food at 25°C with 60% humidity unless otherwise specified. All stocks were preserved or newly constructed by the Tsinghua Fly Center unless otherwise specified. The following stocks were used in our study: Su(H)Gbe-lacZ; *esg*-Gal4, UAS-GFP, tub-Gal80^{ts} (i.e., *esg^{ts}*, a gift from Dr. Zhouhua Li); *pnr*-Gal4/TM3,Sb; UAS-GFP-shRNA (TH00871.N, Sense Oligo: CCCGAAGGTTATGTACAGGAA); a transgenic RNAi

collection for bristle screen; UAS-HP1c-shRNA (TH11826.S, Sense Oligo: TCCGCAAATGCTGATTGACTA); UAS-Notch-shRNA (HMS0001, Sense Oligo: GCGGCGTTAAACAATACCGAA); UAS-HP1c-CDS (TH11574.S); UAS-HP1 γ -CDS (TH11792.S); flySAM-Notch (Notch activation, TH11183.N); yw, hs-FLP; Actin < STOP<GAL4, UAS-GFP/CyO (from Tsinghua Fly Center); yw;;HP1c^{-/-} (HP1c null mutant, from Tsinghua Fly Center); yv;;HP1b^{-/-} (HP1b null mutant, from Tsinghua Fly Center); FRT19A-N^{55e11}/FM7; Sco/CyO (Notch mutant, a gift from Dr. Zhouhua Li); Delta mutant (Bloomington #6300); engrailed-Gal4, UAS-mRFP, NRE-eGFP (BL30729, a gift from Dr. Jian Zhu).

Construction of HP1c overexpression transgenic flies (TH11574.S): full length of HP1c cDNA was amplified using forward primer: 5'-CGGCTAGCATGGTTAAAAACGAGCCCAACTTCG-3' and reverse primer: 5'-GAAGATCTTTATTGATTTCCGCCATGGGC-3'. The PCR product was digested with NheI/BglII and then cloned into the pNP vector (Qiao et al, 2018). A transgenic fly line was produced by injecting this construct into y, sc, v, nanos integrase; attP2 stock and was then screened following standard procedure.

Construction of Notch activation transgenic flies (TH11183.N): sgRNA targeting Notch was amplified using forward primer: 5'-TTCCGGGGAAACTACTCATGCAAG-3' and reverse primer: 5'-AAACCTGCATGAGTAGTTCCCC-3'. After annealing, the sgRNA was cloned into flySAM vector (Jia et al, 2018). Then, the constructed vector was injected into y, sc, v, nanos integrase; attP40 stock and the transgenic line was screened following standard procedure.

Genetics

Pnr-Gal4 virgin females were mated with the corresponding transgenic RNAi males from the high-risk genes' collection, and the phenotypes of bristles were observed and catalogued according to a previous report (Mummary-Widmer et al, 2009). For the gut homeostasis study, we crossed Su(H)Gbe-lacZ; *esg*-Gal4, UAS-GFP, tub-Gal80^{ts} virgin females with the corresponding transgenic RNAi males at 18°C, then transferred the female progeny to 29°C when they hatched, and dissected, immunostained, and observed the midguts from 10-day adult flies. When inducing the RNAi clones in midgut, yw, hs-FLP; actin < STOP<GAL4, UAS-GFP/CyO virgin females were crossed with the corresponding males, and the clones were induced by 45-min heat shock at 37°C 3 days after the female progeny hatched. Then, the flies were transferred to 29°C, and the guts were dissected and immunostained after 10 days. As for the genetic interaction experiments, *Notch* mutant or *Delta* mutant virgin females were, respectively, mated with HP1c null mutant males, and the wings of the offspring males were photographed.

Immunostaining

Immunostaining of *Drosophila* midguts was performed as in previously described protocols (Lin et al, 2008). In brief, midguts were dissected in cold PBS, fixed in a mixture (1:1 v/v) of 4% formaldehyde and *n*-heptane for 20 min, and then washed with methanol twice, followed by washing with PBT (PBS with 0.1% Triton X-100) five times for 15 min each. The samples were first incubated in PBT with 1% goat serum for 1 h at room temperature and then incubated with the appropriate primary antibodies diluted in PBS at 4°C overnight. The samples were washed with PBT five times for

15 min each, incubated with the appropriate secondary antibodies at room temperature for 2 h, followed by incubation with 0.5mg/ml DAPI for 10 min at room temperature. Finally, we washed the samples with PBT five times for 15 min each and mounted them in fluoromount mounting media (Sigma, F4680).

As for the immunostaining of the Notch signaling reporter, NRE-GFP, imaginal wing disks from third-instar larvae were dissected and fixed in 4% paraformaldehyde for 20 min, followed by washing with PBT five times for 15 min each. The samples were then processed by the same method as for midgut. Immunostaining of S2 cells was performed following standard procedure (Peng et al, 2016). Immunostaining of polytene chromosomes was performed according to previous procedure (Stephens et al, 2004).

The following primary antibodies were used: rabbit polyclonal anti-GFP (Abcam ab290, 1:1,000), mouse monoclonal anti-GFP (Roche 1814460, 1:50), rabbit anti-beta-galactosidase (Cappel 55976, 1:1,000), mouse monoclonal anti-Prospero (Abcam ab196361, 1:200), mouse monoclonal anti-HA (Abmart 26D11, 1:500), rabbit polyclonal anti-cleaved caspase-3 (Cell Signaling 9661, 1:200). Various secondary antibodies (Jackson ImmunoResearch Laboratories) conjugated with FITC or TRITC were used at 1:200.

Image acquisition and analysis

Immunostaining images were obtained using an inverted Zeiss LSM780 or Zeiss LSM880 confocal microscope fitted with a UV laser and processed (measured and analyzed) using the Zeiss program (Zeiss Company, version 2012). Other images were captured with a Leica MZ16 FA microscope and processed with ImageJ or Photo-shop Microsoft.

Cell quantity and clonal composition were analyzed by taking stacks from ROIs of posterior midguts. Number of progenitor cells was determined by *esg*-GFP. Number of EBs was determined by Su(H)Gbe-lacZ marker. Number of ISCs was calculated by removing number of EBs from number of *esg*-GFP⁺ cells. Number of ee cells was determined by Prospero marker.

Yeast two-hybrid analysis

We used the Matchmaker® Gold Yeast Two-Hybrid System of Clontech. Full-length HP1c cDNA was cloned into pGBKT7 vector and transformed into Y2HGold yeast to serve as bait. Then, we separately cloned the key components of the Notch signaling pathway, including Notch, Notch intracellular domain (NICD), Su(H), Hairless, and Mastermind (Mam), into pGADT7 vector and transformed them into Y187 yeast to use as prey. Next, we separately mated the prey-containing Y187 with HP1c-containing Y2HGold and observed the growth conditions of resulting diploid cells expressing both proteins on the quadruple dropout medium (QDO), i.e., SD/-Leu/-Trp/-His/-Ade, as well as on the QDO supplied with AbA and X- α -Gal, to screen their interactions with HP1c. pGBKT7-53 (encodes Gal4 DNA-BD fused with murine p53) mated with pGADT7-T (encodes Gal4 AD fused with SV40 large T-antigen) was used as positive control. pGBKT7-Lam (encodes Gal4 BD fused with lamin) mated with pGADT7-T was used as negative control. Further validation of the interaction between HP1c and Su(H) on the contrary orientation, and the interactions between the domains on both orientations, were carried out by the same procedure.

ChIP-qPCR

S2 cells (transfected with the corresponding vectors, which were the same as in the DamID or NRE reporter experiments) were harvested 48 h after seeding (transfection). Then, the samples were processed as in a previous report (Kessler *et al*, 2015) to get the immunoprecipitated chromatin for further qPCR analysis. Triplicated dishes of cells were used as repeated trials, and control samples were always used for normalization.

To perform the ChIP, the following antibodies were used: rabbit polyclonal anti-HP1c (novus 53070002, 1:500), rabbit polyclonal anti-RFP (MBL PM005, 1:1,000), anti-Flag (Abmart M20008, 1:100), anti-HA (Abmart 26D11, 1:100). Primers used in ChIP-qPCR are shown as below.

Pgm: 5'-GGGACAATAGTAGATAACTGG-3'
5'-CAATTTCCACCGTTAGCGAC-3'
GAPDH: 5'-TTGGCGCCACAACCTGCTCAC-3'
5'-ACTTTGGAGCGTTGCATCCC-3'
Rp49: 5'-TACAGGCCCAAGATCGTGAAG-3'
5'-GACGCACTCTGTGTCGATACC-3'
E(spl)m2: 5'-TCCAGCGGGCTCACCTCTC-3'
5'-GCTGCGCCGGCTCGCTCAT-3'
E(spl)mβ: 5'-GCTCGCACTACTGTCCAGT-3'
5'-CTCGCGTAATCCACAGTCGC-3'
Hairy: 5'-GTTAGCAGAGCCAGCAGAG-3'
5'-CCACACGACCGCACCAATAC-3'

DamID

DamID in S2 cells was performed based on previous targeted DamID, named TaDa (Marshall *et al*, 2016), to detect the binding of HP1c at target gene sites. The primers whose PCR products contained CTAG Dam methylation site(s) were used for PCR analysis (same primers are used as ChIP-qPCR assay). To construct the Dam vector, mCherry was amplified (forward primer: 5'-TCTGTTTCAATTTAAAGCTTGC CACCATGGTGAGCAAG-3'; reverse primer: 5'-TTCTTCATGTTAT TACTTGTACAGCTCGTCCATG-3') from our laboratory's stock vector, and Dam was amplified (forward primer: 5'-AAGTAATAACA TGAAGAAAAATCGCGCTTTTTTGAAG-3'; reverse primer: 5'-CGAA CCGCGGGCCTCTAGTTATCTAGATGCGCGGCTTTTTTCGCGGGT GAAACGAC-3') from genome DNA of *E. coli* (*Escherichia coli*). Then, the PCR products were cloned into pIB vector using the Hieff Clone One-Step Cloning Kit (Yeasen, 10911-A), to form the pIB-Dam mock vector. Afterward, HP1c was amplified (forward primer: 5'-AAA AAGCCGGCGCATCTAGAGTAAAAACGAGCCCAACTTC-3'; reverse primer: 5'-GGGCCCTCTAGTTATCTAGATTACTTATCGTCGTCATCC TTGT-3') from wild-type *Drosophila* cDNA and then cloned into XbaI-digested pIB-Dam using the Hieff Clone One-Step Cloning Kit (Yeasen, 10911-A), to form the pIB-Dam-HP1c vector.

Next, pIB-Dam and pIB-Dam-HP1c were transfected into S2 cells together with other plasmids required for experiments (such as pAc-GFP, pAc-NICD, etc.), the cells were harvested and the genome was extracted after 24 h. Subsequently, 1 μg genomic DNA was taken out and digested with DpnII (37°C, overnight) to cut off the unmethylated GATC site. Finally, qPCR primers flanking GATC site(s) and near the transcription initiation site (TSS) of target genes were designed and applied in a qPCR reaction. pAc-GFP and pAc-NICD were constructed

by amplifying GFP or NICD CDS from the corresponding cDNA and then cloning them into pAc5.1A vector (a gift from Professor Renjie Jiao). Specifically, as for the pAc-GFP vector, GFP was amplified (forward primer: 5'-CGGAATTCACCATGGTGAGCAAGGGCGAGGAG-3'; reverse primer: 5'-GCTCTAGATCATTACTTGTACAGCTCGTCCATG-3') from our laboratory's stock vector and then cloned into EcoRI/XbaI-digested pAc5.1A. As for the pAc-NICD vector, NICD was amplified (forward primer: 5'-CGGAATTCACCATGGTCTTGAGTACG CAAAG-3'; reverse primer: 5'-GCTCTAGATCAGCGGAAATGACCGT CGGC-3') from wild-type *Drosophila* cDNA and then cloned into EcoRI/XbaI-digested pAc5.1A.

Notch reporter assays in S2 cells

To get an efficient, observable, and sensitive Notch signaling-specific reporter system, we combined Notch responsive element (NRE, i.e., Su(H)Gbe, containing four Su(H) binding sites) with either eGFP or luciferase, to develop two Notch reporters that work well in S2 cells. First, NRE was annealed from forward primer 5'-GAT CCGTGGCGTGGGAACCGAGCTGAAAGTAAGTTTCTCACACAATAC TAGTCTCGCATAACCGTTTCCAAGA-3' and reverse primer 5'-CT AGTCTTGGAAACCGGTTATGCGAGACTAGTATTGTGTGAGAACT TACTTTACGCTCGGTTCCCACGCCACG-3' and then cloned into the SpeI/BamHI-digested (to remove the U6b: sgRNA elements) sgRNA2.0 luciferase reporter vector (Jia *et al*, 2018) to form the NRE-luciferase vector. Next, this vector was digested with XhoI/KpnI (to remove firefly luciferase) and further introduced to an eGFP (forward primer: 5'-AAGATCCTCTAGCTGGTACTTACTTGT ACAGCTCGTCCATG-3'; reverse primer: 5'-AATAGGGAATTGGCTC GAGACCATGGTGAGCAAGGGC-3') that was amplified from our laboratory's stock vector, to fulfill the NRE-GFP vector. When using this assay, S2 cells were transfected with NRE-GFP/NRE-luciferase vector, while other vectors including either mock pAc5.1A or pAc-gene shRNA were respectively co-transfected, to measure Notch signaling activity.

The pAc-gene shRNA vectors were constructed as follows. First, shRNAs were annealed from forward and reverse primers and cloned into pNP vector following previous procedure (Qiao *et al*, 2018). Then, PCR products amplified (forward primer: 5'-AGACC CCGGATCGGGGTACCTAGAAAACATCCATAAAAACATCC-3'; reverse primer: 5'-ATCTTATCATGTCTGGATCCATATGTCCACTCTAGTAAT TCAGT-3') from pNP vectors were cloned into BamHI/KpnI-digested pAc5.1A using the Hieff Clone One-Step Cloning Kit (Yeasen, 10911-A).

The sense oligos of the shRNAs targeting the genes were as follows:

Hairless: 5'-ATGTTTCATACTAGTAGTCTA-3'
Su(H): 5'-CAGCAACAACAACAACAACA-3'
dSir2: 5'-AAGAGGAAAGATCACACAATA-3'
HP1c: 5'-TCCGCAAATGCTGATTGACTA-3'

pAc-NICD was the same vector as used in the DamID experiments.

RT-qPCR

Twenty pairs of imaginal wing disks from third-instar larvae of control, HP1c KD, and HP1c mutant flies were dissected. Then, total RNAs were extracted using AxyPrep™ Multisource Total RNA Miniprep Kit (Axygen AP-MN-MS-RNA-250) following the

manufacturer's instructions. RNA was retro-transcribed using the GoldScript cDNA Synthesis Kit (Invitrogen c81401190) following the manufacturer's instructions. Real-time PCR was performed using SYBR[®] Premix Ex Taq[™] (Takara RR420A). Normalization was performed against the control gene rp49, and then, fold changes of RNA levels were represented relative to that of control. Primers used are shown as below.

Rp49: 5'-TACAGGCCCAAGATCGTGAAG-3'
 5'-GACGCACTCTGTGTCGATACC-3'
 HP1c: 5'-GGACAAGCGCATTACCAGC-3'
 5'-ACTCCTCGAATTTCTGGATGAGA-3'
 E(spl)m2: 5'-CTGGATACGAAAAACCTGACAGC-3'
 5'-CGCCGTGTTGACTTTGAGT-3'
 HLHm5: 5'-TTGGACACCTTGAAGACCTTGG-3'
 5'-CTGCTGCTTGACGACCTGTTG-3'
 Hairy: 5'-GACTCTGATTCTGGATGCCAC-3'
 5'-CTAACCTCGTTCACACAGTCG-3'

Co-immunoprecipitation

Drosophila S2 cells were cultured at 25°C in Schneider's *Drosophila* medium (Invitrogen 21720024) containing 10% FBS (PAA A005N). Cells cultured in 6-well dishes were transfected with appropriate expression constructs using X-tremeGENE HP DNA Transfection Reagent (Roche 06366236001). Cells were harvested after 48 h and total protein extract was prepared using lysis buffer (NP-40). Then, lysates were incubated in mixture containing 3 µl rabbit anti-GFP (Abcam ab290) or mouse anti-Flag (Abmart M20008) antibody and Protein A + G Agarose beads (Beyotime P2012) overnight at 4°C. After washing in lysis buffer for five times, immunoprecipitates were boiled in 5× SDS loading buffer to dissociate proteins from beads. The following antibodies were used for Western blots to detect co-immunoprecipitated proteins: mouse monoclonal anti-GFP (Abmart M20004, 1:5,000), mouse monoclonal anti-Flag (Abmart M20008, 1:2,000), rabbit anti-HP1c (novus 53070002, 1:5,000).

Integrative network and omics analysis

In silico prediction, high-risk genes for gastrointestinal cancer were predicted by our network-based algorithm CIPHER, a genome-wide gene–phenotype association predictor according to network correlations between disease phenotypes and corresponding genes from OMIM database (<https://omim.org/>; Wu *et al*, 2008). It is regarded as a representative method for disease gene prediction (Wu *et al*, 2008; Barabasi *et al*, 2011). Firstly, we inputted the gastrointestinal inflammation and cancer terms (MIM 114500 and MIM 613659) into CIPHER algorithm. Next, top 5% predicted disease genes of connected in the molecular network are selected. Taking advantage of the prediction results, we analyzed the tumor-related functions of high-risk genes. Furthermore, we explore the molecular role of these genes in tumorigenesis by screening in *Drosophila* notum bristle. TCGA transcriptome datasets and clinical information (colon adenocarcinoma (COAD) and stomach adenocarcinoma (STAD)) were obtained from the UCSC Cancer Genomics (<https://genome-cancer.ucsc.edu/proj/site/hgHeatmap/>). The analysis pipeline of

differential gene expression referred to the literature (Tang *et al*, 2017).

Statistics and reproducibility

GraphPad Prism and Excel were used to calculate the mean, the SEM, or the s.d. for all the column diagram data, as well as the statistical analysis. The *n* of each test and detailed statistical analysis method is shown in the figure legends.

Data availability

The data that support the findings of this study are available from the corresponding author upon reasonable request. No large primary datasets have been generated or deposited.

Expanded View for this article is available online.

Acknowledgements

We thank Dr. Ferran Azorín for the anti-HP1c antibody and Dr. Xiaohang Yang for the anti-pros antibody. We thank Dr. José Carlos Pastor-Pareja and Dr. Yi Zhong for their advice on the manuscript. Besides we thank Dr. Zhouhua Li, Dr. Jian Zhu, and Dr. Rongwen Xi for providing *Drosophila* lines. This work was supported by the National Natural Science Foundation of China (31872818, 32070640, 31571320, 31801079, 6201101081), and the National Key Technology Research and Development Program of the Ministry of Science and Technology of the People's Republic of China (2017YFA0103300, 2016YFE0113700, 2015BAI09B03).

Author contributions

J-QN and F-LS designed the experiment. JS, XiaW, R-GX, DM, DS, YQ, YH, LZ, PP, XK, RZ, YJ, XL, YL, YW, QC, and L-PL performed the experiments. JS, XiaW, R-GX, XinW, J-YJ, ZC, ZW, QL, SL, J-QN, and F-LS performed data analysis. J-QN, JS, YH, XL, YL, and R-GX wrote and revised the manuscript.

Conflict of interest

The authors declare that they have no conflict of interest.

References

- Abel J, Eskeland R, Raffa GD, Kremmer E, Imhof A (2009) *Drosophila* HP1c is regulated by an auto-regulatory feedback loop through its binding partner Woc. *PLoS One* 4: e5089
- Aster JC, Pear WS, Blacklow SC (2017) The varied roles of Notch in cancer. *Ann Rev Pathol* 12: 245–275
- Bannister AJ, Zegerman P, Partridge JF, Miska EA, Thomas JO, Allshire RC, Kouzarides T (2001) Selective recognition of methylated lysine 9 on histone H3 by the HP1 chromo domain. *Nature* 410: 120–124
- Barabasi AL, Gulbahce N, Loscalzo J (2011) Network medicine: a network-based approach to human disease. *Nat Rev Genet* 12: 56–68
- Bedogni B (2014) Notch signaling in melanoma: interacting pathways and stromal influences that enhance Notch targeting. *Pigment Cell & Melanoma Research* 27: 162–168.

- Biteau B, Hochmuth CE, Jasper H (2011) Maintaining tissue homeostasis: dynamic control of somatic stem cell activity. *Cell Stem Cell* 9: 402–411
- Canzio D, Larson A, Narlikar GJ (2014) Mechanisms of functional promiscuity by HP1 proteins. *Trends Cell Biol* 24: 377–386
- Contreras-Cornejo H, Saucedo-Correa G, Oviedo-Boyso J, Valdez-Alarcon JJ, Baizabal-Aguirre VM, Cajero-Juarez M, Bravo-Patino A (2016) The CSL proteins, versatile transcription factors and context dependent corepressors of the notch signaling pathway. *Cell Div* 11: 12
- Eissenberg JC, Elgin SCR (2000) The HP1 protein family: getting a grip on chromatin. *Curr Opin Genet Dev* 10: 204–210
- Font-Burgada J, Rossell D, Auer H, Azorin F (2008) *Drosophila* HP1c isoform interacts with the zinc-finger proteins WOC and Relative-of-WOC to regulate gene expression. *Genes Dev* 22: 3007–3023
- Fre S, Bardin A, Robine S, Louvard D (2011) Notch signaling in intestinal homeostasis across species: the cases of *Drosophila*, Zebrafish and the mouse. *Exp Cell Res* 317: 2740–2747
- Geissler K, Zach O (2012) Pathways involved in *Drosophila* and human cancer development: the Notch, Hedgehog, Wingless, Runt, and Trithorax pathway. *Ann Hematol* 91: 645–669
- Gomez-Lamarca MJ, Falo-Sanjuan J, Stojnic R, Abdul Rehman S, Muresan L, Jones ML, Pillidge Z, Cerda-Moya G, Yuan Z, Baloul S et al (2018) Activation of the Notch signaling pathway in vivo elicits changes in CSL nuclear dynamics. *Dev Cell* 44: 611–623
- Goulas S, Conder R, Knoblich JA (2012) The Par complex and integrins direct asymmetric cell division in adult intestinal stem cells. *Cell Stem Cell* 11: 529–540
- Guarani V, Deflorian G, Franco CA, Kruger M, Phng LK, Bentley K, Toussaint L, Dequiedt F, Mostoslavsky R, Schmidt MH et al (2011) Acetylation-dependent regulation of endothelial Notch signalling by the SIRT1 deacetylase. *Nature* 473: 234–238
- Han H, Fan J, Xiong Y, Wu W, Lu Y, Zhang L, Zhao Y (2016) Chi and dLMO function antagonistically on Notch signaling through directly regulation of fng transcription. *Sci Rep* 6: 18937
- Jia Y, Xu RG, Ren X, Ewen-Campen B, Rajakumar R, Zirin J, Yang-Zhou D, Zhu R, Wang F, Mao D et al (2018) Next-generation CRISPR/Cas9 transcriptional activation in *Drosophila* using flySAM. *Proc Natl Acad Sci USA* 115: 4719–4724
- Jiang H, Edgar BA (2011) Intestinal stem cells in the adult *Drosophila* midgut. *Exp Cell Res* 317: 2780–2788
- Kessler R, Tisserand J, Font-Burgada J, Reina O, Coch L, Attolini CS, Garcia-Bassets I, Azorin F (2015) dDsk2 regulates H2Bub1 and RNA polymerase II pausing at dHP1c complex target genes. *Nat Commun* 6: 7049
- Koch U, Radtke F (2007) Notch and cancer: a double-edged sword. *Cell Mol Life Sci* 64: 2746–2762
- Kwon SH, Florens L, Swanson SK, Washburn MP, Abmayr SM, Workman JL (2010) Heterochromatin protein 1 (HP1) connects the FACT histone chaperone complex to the phosphorylated CTD of RNA polymerase II. *Genes Dev* 24: 2133–2145
- Kwon SH, Workman JL (2011) HP1c casts light on dark matter. *Cell Cycle* 10: 625–630
- Lachner M, Carroll DO, Rea S, Mechtler K, Jenuwein T (2001) Selective recognition of methylated lysine 9 on histone H3 by the HP1 chromo domain. *Nature* 410: 116–120
- Lemaitre B, Miguel-Aliaga I (2013) The digestive tract of *Drosophila melanogaster*. *Annu Rev Genet* 47: 377–404
- Lin G, Xu N, Xi R (2008) Paracrine Wingless signalling controls self-renewal of *Drosophila* intestinal stem cells. *Nature* 455: 1119–1123
- Maier D, Praxenthaler H, Schulz A, Preiss A (2013) Gain of function notch phenotypes associated with ectopic expression of the Su(H) C-terminal domain illustrate separability of Notch and hairless-mediated activities. *PLoS One* 8: e81578
- Marshall OJ, Southall TD, Cheetham SW, Brand AH (2016) Cell-type-specific profiling of protein-DNA interactions without cell isolation using targeted DamID with next-generation sequencing. *Nat Protoc* 11: 1586–1598
- Micchelli CA, Perrimon N (2006) Evidence that stem cells reside in the adult *Drosophila* midgut epithelium. *Nature* 439: 475–479
- Mulligan P, Yang F, Di Stefano L, Ji JY, Ouyang J, Nishikawa JL, Toiber D, Kulkarni M, Wang Q, Najafi-Shoushtari SH et al (2011) A SIRT1-LSD1 corepressor complex regulates Notch target gene expression and development. *Mol Cell* 42: 689–699
- Mummery-Widmer JL, Yamazaki M, Stoeger T, Novatchkova M, Bhalerao S, Chen D, Dietzl G, Dickson BJ, Knoblich JA (2009) Genome-wide analysis of Notch signalling in *Drosophila* by transgenic RNAi. *Nature* 458: 987–U959
- Nagel AC, Szawinski J, Zimmermann M, Preiss A (2016) *Drosophila* cyclin G is a regulator of the Notch signalling pathway during wing development. *PLoS One* 11: e0151477
- Nowell CS, Radtke F (2017) Notch as a tumour suppressor. *Nat Rev Cancer* 17: 145–159
- Ohlstein B, Spradling A (2006) The adult *Drosophila* posterior midgut is maintained by pluripotent stem cells. *Nature* 439: 470–474
- Ohlstein B, Spradling A (2007) Multipotent *Drosophila* intestinal stem cells specify daughter cell fates by differential notch signaling. *Science* 315: 988–992
- Pasco MY, Loudhaief R, Gallet A (2015) The cellular homeostasis of the gut: what the *Drosophila* model points out. *Histol Histopathol* 30: 277–292
- Peng Q, Wang Y, Li M, Yuan D, Xu M, Li C, Gong Z, Jiao R, Liu L (2016) cGMP-Dependent protein kinase encoded by foraging regulates motor axon guidance in *Drosophila* by suppressing lola function. *J Neurosci* 36: 4635–4646
- Perdigoto CN, Schweisguth F, Bardin AJ (2011) Distinct levels of Notch activity for commitment and terminal differentiation of stem cells in the adult fly intestine. *Development* 138: 4585–4595
- Qiao HH, Wang F, Xu RG, Sun J, Zhu R, Mao D, Ren X, Wang X, Jia Y, Peng P et al (2018) An efficient and multiple target transgenic RNAi technique with low toxicity in *Drosophila*. *Nat Commun* 9: 4160
- Reedijk M, Odorcic S, Chang L, Zhang H, Miller N, McCreedy DR, Lockwood G, Egan SE (2005) High-level coexpression of JAG1 and NOTCH1 is observed in human breast cancer and is associated with poor overall survival. *Cancer* 95: 8530–8537
- Ren X, Holsteens K, Li H, Sun J, Zhang Y, Liu L-P, Liu Q, Ni J-Q (2017) Genome editing in *Drosophila melanogaster*: from basic genome engineering to the multipurpose CRISPR-Cas9 system. *Sci China Life Sci* 60: 476–489
- Ren X, Sun J, Housden BE, Hu Y, Roesel C, Lin S, Liu L-P, Yang Z, Mao D, Sun L et al (2013) Optimized gene editing technology for *Drosophila melanogaster* using germ line-specific Cas9. *Proc Natl Acad Sci USA* 110: 19012–19017
- Ren X, Yang Z, Xu J, Sun J, Mao D, Hu Y, Yang S-J, Qiao H-H, Wang X, Hu Q et al (2014) Enhanced specificity and efficiency of the CRISPR/Cas9 system with optimized sgRNA parameters in *Drosophila*. *Cell Rep* 9: 1151–1162
- Ryu HW, Lee DH, Florens L, Swanson SK, Washburn MP, Kwon SH (2014) Analysis of the heterochromatin protein 1 (HP1) interactome in *Drosophila*. *J Proteomics* 102: 137–147
- Saj A, Arziman Z, Stempfle D, van Belle W, Sauder U, Horn T, Duerrenberger M, Paro R, Boutros M, Merdes G (2010) A combined ex vivo and in vivo RNAi screen for Notch regulators in *Drosophila* reveals an extensive Notch interaction network. *Dev Cell* 18: 862–876

- Stephens GE, Craig CA, Li YH, Wallrath LL, Elgin SCR (2004) Immunofluorescent staining of polytene chromosomes: exploiting genetic tools. *Chromatin Chromatin Remodel Enzymes Pt B* 376: 372–393
- Sun J, Wei HM, Xu J, Chang JF, Yang Z, Ren X, Lv WW, Liu LP, Pan LX, Wang X et al (2015) Histone H1-mediated epigenetic regulation controls germline stem cell self-renewal by modulating H4K16 acetylation. *Nat Commun* 6: 8856
- Tang Z, Li C, Kang B, Gao G, Li C, Zhang Z (2017) GEPIA: a web server for cancer and normal gene expression profiling and interactive analyses. *Nucleic Acids Res* 45: W98–W102
- Vermaak D, Malik HS (2009) Multiple roles for heterochromatin protein 1 genes in *Drosophila*. *Annu Rev Genet* 43: 467–492
- Wu X, Jiang R, Zhang MQ, Li S (2008) Network-based global inference of human disease genes. *Mol Syst Biol* 4: 189